# Co-optimized Bidding Strategy of an Integrated Wind-Thermal-Photovoltaic System in Deregulated Electricity Market Under Uncertainties

Hooman Khaloie[1], Amir Abdollahi[1], Miadreza Shafie-khah[2], Pierluigi Siano[3], Sayyad Nojavan[4], Amjad Anvari-Moghaddam[5], João P.S. Catalão[6]

*(1) Department of Electrical Engineering, Shahid Bahonar University of Kerman, Kerman, Iran*

*(2) School of Technology and Innovations, University of Vaasa, 65200 Vaasa, Finland*

*(3) Department of Management & Innovation Systems, University of Salerno, Fisciano, Italy*

*(4) Department of Electrical Engineering, University of Bonab, Bonab, Iran*

*(5) Department of Energy Technology, Aalborg University, Aalborg, Denmark*

*(6) Faculty of Engineering of the University of Porto and INESC TEC, 4200-465, Porto, Portugal*

**Abstract**

Clean Energy sources, such as wind and solar, have become an inseparable part of today's power grids. However, the intermittent nature of these sources has become the greatest challenge for their owners, which makes the bidding in the restructured electricity market more challenging. Hence, the main goal of this paper is to propose a novel multi-objective bidding strategy framework for a wind-thermal-photovoltaic system in the deregulated electricity market for the first time. Contrary to the existing bidding models, in the proposed model, two objective functions are taken into account that the first one copes with profit maximization while the second objective function concerns with emission minimization of thermal units. The proposed multi-objective optimization problem is solved using the weighted sum approach. The uncertainties associated with electricity market prices and the output power of renewable energy sources are characterized by a set of scenarios. Ultimately, in order to select the best-compromised solution among the obtained Pareto optimal solutions, two diverse approaches are applied. The proposed bidding strategy problem is being formulated and examined in various modes of joint and disjoint operation of dispatchable and non-dispatchable energy sources. Simulation results illustrate that not only the integrated participation of these resources increases the producer's expected profits but also decreases the amount of the produced pollution by the thermal units.

*Keywords:* Integrated operation, bidding strategy, Multi-objective optimization, Wind-thermal-Photovoltaic system, weighted-sum technique, Emission trading

---

| | |
|---|---|
| **Nomenclature** | |
| ***Indices*** | |
| t | Period index. |
| g | Index for thermal units. |
| $\omega$ | Scenario index. |
| b | Index for blocks of the generation cost curve and emission curve of thermal units. |
| ***Constants*** | |
| $\pi_\omega$ | Probability of occurrence of scenario $\omega$ |
| $P^{W,Max}$ | Rated wind power output, MW. |
| $P^{PV,Max}$ | Rated PV power output, MW. |
| $STUC(g)$ | Start-up cost of every thermal unit, €/each start-up. |
| $MDT(g)$ | Minimum down-time of every thermal unit, hr. |
| $MUT(g)$ | Minimum up-time of every thermal unit, hr. |
| $RUR(g)$ | Ramp-up rate of every thermal unit, MW/hr. |
| $RDR(g)$ | Ramp-down rate of every thermal unit, MW/hr. |
| $E^{EQ}$ | Emission quota of power producer, lbs. |

| | |
|---|---|
| $P^{Maxb}(b,g)$ | Maximum power output of every thermal unit in $b$th block of the piecewise linear cost function, MW. |
| $P^{Max}(g)$ | Maximum power output of every thermal unit, MW. |
| $P^{Min}(g)$ | Minimum power output of every thermal unit, MW. |
| $PS^{Max}(g)$ | Maximum capacity of every thermal unit for participating in the spinning reserve market, MW. |
| $NC(g)$ | No-load generating cost of every thermal unit, €/hr. |
| $IC(b,g)$ | Incremental generating cost of $b$th block of unit g, €/MWhr. |
| $E(q,b,g)$ | Slope of block $b$ in emission group $q$ of every thermal unit, $lbs$/MWhr. |
| $EMG$ | Emission group including $NO_X$ and $SO_2$. |
| $STURL(g)$ | Start-up ramp bound of every thermal unit, MW/hr. |
| $STDRL(g)$ | Shut-down ramp bound of every thermal unit $g$, MW/hr. |
| $a_g, b_g, c_g$ | Coefficients of thermal generation cost function. |
| $\alpha_g, \beta_g, \gamma_g$ | Emission coefficients of thermal unit $g$. |
| $N_T$ | Number of periods. |
| $N_G$ | Number of thermal units. |
| $N_\Omega$ | Number of scenarios. |
| $N_b$ | Number of segments of the production cost and emission curve. |
| $\lambda^{EM}$ | Emission market price, €/lbs. |
| ***Variables*** | |
| $\lambda^E(t,\omega)$ | Price of day-ahead energy market, €/MW. |
| $\lambda^S(t,\omega)$ | Price of spinning reserve market, €/MW. |
| $P^{th,S}(t,\omega)$ | Optimal bid of thermal units in the spinning reserve market, MW. |
| $P^{th,E}(t,\omega)$ | Optimal bid of thermal units in the day-ahead energy market, MW. |
| $P^W(t,\omega)$ | Optimal bid of wind power plant in the day-ahead energy market, MW. |
| $P^{PV}(t,\omega)$ | Optimal bid of PV system in the day-ahead energy market, MW. |
| $P^{th,Ac}(t,\omega)$ | Actual power output of thermal units, MW. |
| $P^{W,F}(t,\omega)$ | Realized power output of wind power plant, MW. |
| $P^{PV,F}(t,\omega)$ | Realized power output of PV system, MW. |
| $P^C(t,\omega)$ | Joint energy offer of the all energy resources in the day-ahead energy market, MW. |

| | |
|---|---|
| $\Delta^+(t,\omega)$ | Imbalance-up, MW. |
| $\Delta^-(t,\omega)$ | Imbalance-down, MW. |
| $STU(g,t,\omega)$ | Start-up cost of every thermal unit, €. |
| $C(g,t,\omega)$ | Generation cost of every thermal unit, €. |
| $EG(b,g,t,\omega)$ | Produced power of thermal units through the $b$th block of the piecewise linear cost function for participating in the day-ahead energy market, MW. |
| $ES(g,t,\omega)$ | Power offer of every thermal unit in the spinning reserve market, MW. |
| $ET(g,t,\omega)$ | Total power offer by every thermal unit in all selected markets, MW. |
| $u(g,t,\omega)$ | Binary variable which indicates acceptance situation of every thermal unit in the day-ahead energy market. |
| $x(g,t,\omega)$ | Binary variable which indicates start-up situation of thermal units in the day-ahead energy market. |
| $y(g,t,\omega)$ | Binary variable which indicates shut-down situation of thermal units in the day-ahead energy market. |
| $r^+(t,\omega)$ | Imbalance penalty for over-generation as multiplier of energy price |
| $r^-(t,\omega)$ | Imbalance penalty for under-generation as multiplier of energy price |

## 1. Introduction

### *1.1. Motivation and Aim*

Nowadays, a wide range of power system issues is affected by the presence of renewable energy resources. With the growth of industries and communities, the request for supplying customers demand is rising day-to-day [1]. In this regard, conventional energy sources such as coal, gas and nuclear, as well as renewable energy sources, e.g., hydro, wind and solar, are the two main options for governments to supply the required electricity of communities [2]. Generally, the rising cost of fossil fuels and attention to environmental concerns can be mentioned as the main reasons for the desire of diverse communities to augment the penetration of renewable energy sources [3]. Briefly, sustainability, environmentally friendly, reducing fossil fuel consumption, and low maintenance costs are among the reasons for increasing the interest of various communities in renewable energy sources [4]. Despite many subsidies that governments have devoted to renewable energy developers, we will witness a significant increase in investments in this sector [5]-[6]. On the other hand, the existence of subsidies will not guarantee the profits of investors. Hence, the deregulated electricity market lay the groundwork for both producers and consumers to devise the best possible strategy for themselves. Consequently, renewable energy sources owned by generation companies (GenCos)/large consumers must design the most profitable bidding strategy by participating in various electricity markets.

### *1.2. Literature Review*

The problem of optimal bidding strategy/self-scheduling has attracted the attention of many researchers so far [7]-[22]. A bidding structure based on the joint implementation of stochastic and robust uncertainty modeling approaches for an industrial consumer has been addressed in [7]. Likewise, in [8], the authors conducted a stochastic-robust optimization-based framework for a bidding strategy of a large consumer in a deregulated electricity market. In both papers [7] and [8], the uncertainty of load is addressed by the specified range, and the uncertainty related to renewable productions and market prices are modeled via independent scenarios. A self-scheduling model for the participation of a sample microgrid containing plug-in electric vehicles, wind turbines, and fuel cell units has been developed in [9]. In [10], authors have proposed a coordinated self-production and load-scheduling framework for an industrial plant in joint electricity and carbon emission markets. A hybrid probabilistic-possibilistic technique has been employed in [11] to cope with the uncertainties in the self-scheduling of thermal units. In [12], authors have focused on presenting a bi-objective self-scheduling structure for a typical factory as a large consumer. In [13], a risk-constrained self-scheduling model for a real virtual power plant in Iran has been suggested.

Integrated energy resources scheduling is one of the most challenging problems in the electrical power system which has attracted much attention. Wind power generation as one of the most favorite organ of integrated energy resources has been widely considered alongside other production resources such as thermal, hydro, solar, and pumped storage power plants. In [14], the authors present an integrated self-scheduling model for a wind-pumped-storage system while the uncertainty of wind power generation is modeled by a neural network based technique. Authors illustrated that presenting a coordinated bidding strategy of both resources can remarkably raise their profitability. A critical shortage of this work is that the authors have not modeled the uncertainty associated with electricity market prices. Authors in [15], presented a linear programming framework for self-scheduling of a hydro-thermal system, whereas the electricity market prices and forced outages of generating units have been considered uncertain as the uncertain sources. Likewise, the investigation of integrated wind and thermal energy sources in the context of the bidding strategy problem have been accomplished in [16]-[18]. The ultimate goal of all these three works is to prove the profitability of integrated scheduling compared to non-integrated one. In [19], a risk-based bidding framework for a wind-thermal-pumped storage system is presented.

Contrary to the mentioned studies, the bi-objective scheduling of integrated energy systems with the aim of minimizing pollution emission has also been considered by researchers [20]-[21]. In [20], a bi-objective microgrid self-scheduling model is presented in which the microgrid cost and emission minimizations are taking into account. A multi-objective self-scheduling model for a hydro-thermal system considering joint energy and ancillary services markets is proposed in [21]. In [22], a multi-objective economic dispatch model for pumped-hydro-thermal systems is presented in which the normal boundary intersection is utilized to achieve the Pareto optimal solutions. The taxonomy of reviewed papers [7]-[22] based on different aspects of their works has been listed in Table 1.

Table 1 is placed here

### 1.3. Contributions

According to the reviewed papers in subsection 1.2 and the specified characteristics for each paper in Table 1, this paper focuses on presenting a novel bi-objective bidding strategy of a wind-thermal-photovoltaic system in the energy and spinning reserve markets. To the best of author's knowledge, this work proposes the most comprehensive study in the context of multi-objective and single-objective coordinated bidding strategy of wind, thermal and photovoltaic units in the literature, so the major contributions of this paper are:

- Presenting a comprehensive coordinated mathematical formulation for the multi-objective bidding strategy of all existing sources.
- Proposing a novel bi-objective bidding strategy for a wind-thermal-photovoltaic (WTPV) system participating in the energy and spinning reserve markets. The process of profit maximization and emission minimization are concurrently accomplished while the uncertainty arising from day-ahead energy, spinning reserve, and imbalance prices along with the output power of renewable energy resources are addressed in the proposed framework.
- An efficient solution method, namely, the hybrid weighted sum method and fuzzy satisfying approach, is introduced as the solution methodology of the bi-objective bidding strategy problem
- A decision-making scheme based on the preferences of decision-maker is suggested in the bidding strategy problem to select the most favored solution.
- Proposing an additional pattern based on the emission trading concept for an emission-constrained WTPV power producer to select the best possible strategy.

## 2. Problem formulation

The multi-objective bidding strategy problem of a WTPV system is formulated as a stochastic mixed integer programming (MIP) which maximizing the expected profit of WTPV system and minimizing the expected emission arising from thermal units are considered as two distinct objective functions of the decision-maker. In the following subsections, separate objective functions of the bi-objective bidding strategy problem will be thoroughly explained.

### 2.1. First objective function: Maximizing expected profit

The primary purpose of the WTPV system is to maximize its profits through participation in diverse electricity markets in the 24-hour scheduled horizon. In the coordinated bidding structure, a single offering package will be offered to the energy market from all existing energy resources while the offering package of power producer in the spinning reserve market exclusively contains the participation of thermal units in this market. The first objective function of the power producer for the coordinated operation of all resources is formulated as follows:

$$
\begin{aligned}
\text{Max } F_1^C = & \sum_{\omega=1}^{N_\Omega} \pi_\omega \times [\sum_{t=1}^{T} (\lambda^E(t,\omega) P^{th,E}(t,w) + \lambda^E(t,\omega) P^W(t,w) \\
& + \lambda^E(t,\omega) P^{PV}(t,w) + \lambda^S(t,\omega) P^{th,S}(t,w) \\
& + \lambda^E(t,\omega) r^+(t,\omega) \Delta^+(t,\omega) - \lambda^E(t,\omega) r^-(t,\omega) \Delta^-(t,\omega))] \\
& - \sum_{\omega=1}^{N_\Omega} \pi_\omega \times [\sum_{t=1}^{T} \sum_{g=1}^{N_G} C(g,t,\omega) - \sum_{t=1}^{T} \sum_{g=1}^{N_G} (STU(g,t,\omega))]
\end{aligned} \tag{1}
$$

where the first two lines of (1) represent the expected income of power producer from participating in the day-ahead energy and spinning reserve markets while the third line relates to the imbalances of power producer in the balancing market, finally, the last line refers to the costs of operating and start-up costs of the thermal units. The constraints of the objective function (1) would be categorized into the following groups:

- Coordinated operation constraints: Constraint (2) calculates the final bid of power producer that should be offered to the energy market. Constraints (3)-(6) model the imbalances of the power producer in the balancing market. Restriction (5) limits the positive energy deviations of power producer within the total actual power output of all three sources while constraint (6) ensures that the negative energy deviations should not exceed the maximum capacity of renewable energy sources plus the maximum available capacity of thermal units. Equations (7) and (8) represent the upper and lower bounds of the scheduled power of renewable energy sources. Constraint (9)-(10) and (11)-(12) are the non-decreasing and non-anticipativity settings for the offering packages in the energy and spinning reserve markets, respectively.

$$P^{C}(t,\omega) = P^{th,E}(t,w) + P^{W}(t,w) + P^{PV}(t,w) \quad \forall t, \forall \omega \tag{2}$$

$$\Delta(t,w) = P^{PV,F}(t,\omega) + P^{W,F}(t,\omega) + P^{th,Ac}(t,\omega) - P^{C}(t,w), \quad \forall t, \forall \omega \tag{3}$$

$$\Delta(t,w) = \Delta^{+}(t,\omega) - \Delta^{-}(t,\omega), \quad \forall t, \forall \omega \tag{4}$$

$$0 \leq \Delta^{+}(t,\omega) \leq P^{PV,F}(t,\omega) + P^{W,F}(t,\omega) + P^{th,Ac}(t,\omega), \quad \forall t, \forall \omega \tag{5}$$

$$0 \leq \Delta^{-}(t,\omega) \leq P^{PV,Max} + P^{W,Max} + \sum_{g=1}^{N_G} P^{Max}(g).u(g,t,\omega), \quad \forall t, \forall \omega \tag{6}$$

$$0 \leq P^{W}(t,w) \leq P^{W,Max}, \quad \forall t, \forall \omega \tag{7}$$

$$0 \leq P^{PV}(t,w) \leq P^{PV,Max}, \quad \forall t, \forall \omega \tag{8}$$

$$P^{C}(t,\omega) \leq P^{C}(t,\widetilde{\omega}), \quad \forall \omega, \widetilde{\omega} : [\lambda^{E}(t,\omega) \leq \lambda^{E}(t,\widetilde{\omega})], \quad \forall t \tag{9}$$

$$P^{th,S}(t,\omega) \leq P^{th,S}(t,\widetilde{\omega}), \quad \forall \omega, \widetilde{\omega} : [\lambda^{S}(t,\omega) \leq \lambda^{S}(t,\widetilde{\omega})], \quad \forall t \tag{10}$$

$$P^{C}(t,\omega) = P^{C}(t,\widetilde{\omega}), \quad \forall \omega, \widetilde{\omega} : [\lambda^{E}(t,\omega) = \lambda^{E}(t,\widetilde{\omega})], \quad \forall t \tag{11}$$

$$P^{th,S}(t,\omega) = P^{th,S}(t,\widetilde{\omega}), \quad \forall \omega, \widetilde{\omega} : [\lambda^{S}(t,\omega) = \lambda^{S}(t,\widetilde{\omega})], \quad \forall t \tag{12}$$

- Thermal units constraints: The generation cost of thermal units for energy delivery is computed through constraint (13). The quadratic cost curve of thermal units makes the problem nonlinear. In order to overcome this issue, many researchers have been approximated this cost curve using various piecewise blocks [20]. In the current paper, these piecewise linearized segments are indexed by letter $b$. Constraint (14) represents the total bid of thermal units in the energy market. Equations (15) and (16) restrict the generated power of thermal units within their minimum and maximum bounds. Constraint (17) calculates total bid of thermal units in the spinning reserve market while equation (18) is implemented to limit the spinning reserve offer of generation facility within their maximum capability in providing upward spinning reserve. Constraints (19) and (20) are fulfilled to restrict the total bids of thermal units in the day-ahead energy and spinning reserve market within their limited operating areas. Constraints (21) is fulfilled to calculate the start-up costs incurred by thermal units during the scheduling horizon. Other technical restrictions of thermal units, as well as the minimum up/down time and the logical relationship between the various status of generation facilities, are enforced by constraints (22)-(24). Finally, the ramp-up and ramp-down limitations, considering the shut-down and start-up ramps of thermal units are modeled by constraints (25)-(26).

$$C(g,t,\omega) = NC(g)u(g,t,\omega) + \sum_{b=1}^{N_b} IC(b,g)EG(b,g,t,\omega), \quad \forall t, \forall \omega \tag{13}$$

$$\sum_{g=1}^{N_G}\sum_{b=1}^{N_b} EG(b,g,t,\omega) = P^{th,E}(t,\omega), \quad \forall t, \forall \omega \tag{14}$$

$$0 \leq EG(b,g,t,\omega) \leq P^{Maxb}(b,g), \quad \forall b, \forall g, \forall t, \forall \omega \tag{15}$$

$$P^{Min}(g)u(g,t,\omega) \leq \sum_{b=1}^{N_b} EG(b,g,t,\omega) \leq P^{Max}(g)u(g,t,\omega), \quad \forall g, \forall t, \forall \omega \tag{16}$$

$$\sum_{g=1}^{N_G} ES(g,t,\omega) = P^{th,S}(t,\omega), \quad \forall t, \forall \omega \tag{17}$$

$$0 \leq ES(g,t,\omega) \leq PS^{Max}(g)u(g,t,\omega), \quad \forall g, \forall t, \forall \omega \tag{18}$$

$$ET(g,t,\omega) = \sum_{b=1}^{N_b} EG(b,g,t,\omega) + ES(g,t,\omega), \quad \forall g, \forall t, \forall \omega \tag{19}$$

$$P^{Min}(g)u(g,t,\omega) \leq ET(g,t,\omega) \leq P^{Max}(g)u(g,t,\omega), \quad \forall g, \forall t, \forall \omega \tag{20}$$

$$0 \leq STU(g,t,\omega) \geq STUC(g)x(g,t,\omega), \quad \forall g, \forall t, \forall \omega \tag{21}$$

$$\sum_{n=t-MUT(g)+1}^{t} x(g,t,\omega) \leq u(g,t,\omega), \quad \forall g, \forall t, \forall \omega \tag{22}$$

$$u(g,t,\omega) + \sum_{n=t-MDT(g)+1}^{t} y(g,t,\omega) \leq 1, \quad \forall g, \forall t, \forall \omega \tag{23}$$

$$u(g,t-1,\omega) - u(g,t,\omega) + x(g,t,\omega) - y(g,t,\omega) = 0, \quad \forall g, \forall t, \forall \omega \tag{24}$$

$$\begin{aligned} \sum_{b=1}^{N_b} EG(b,g,t,\omega) \leq \sum_{b=1}^{N_b} EG(b,g,t-1,\omega) + RUR(g)u(g,t-1,\omega) \\ + STURL(g)x(g,t,\omega), \quad \forall g, \forall t, \forall \omega \end{aligned} \tag{25}$$

$$\begin{aligned} \sum_{b=1}^{N_b} EG(b,g,t-1,\omega) \leq \sum_{b=1}^{N_b} EG(b,g,t,\omega) + RDR(g)u(g,t,\omega) \\ + STDRL(g)y(g,t,\omega), \quad \forall g, \forall t, \forall \omega \end{aligned} \tag{26}$$

### 2.2. Second objective function: Minimizing expected emission

The second objective function of the power producer in the proposed structure is emission minimization. In fact, due to the worldwide rising concerns about environmental issues, minimizing the produced pollution by thermal units is consistently considered as one of the objective functions of the power producers in the optimization process. The linear form of this objective function would be as follows:

$$\text{Min } \; F_2^{th} = \sum_{\omega=1}^{N_\Omega} \pi_\omega [\times \sum_{q=1}^{EMG} \sum_{g=1}^{N_G} \sum_{b=1}^{N_b} E(q,b,g) EG(b,g,t,\omega)] \tag{27}$$

It is worth to note that in order to take advantage of linear programming in the proposed structure, the emission functions of thermal units, which generally have a quadratic form, are approximated by some piecewise linearized blocks. In the current paper, the $SO_2$ and $NO_X$ are taken into consideration as the primary sources of emission [21].

In this paper, three different bidding strategies, including the coordinated and uncoordinated operation of various energy sources, are considered to thoroughly examine the productivity of the proposed structure. Fig. 1 shows these three different bidding strategies with their determinant constraints. These three trading strategies are designed to exhaustively assess the multi-objective bidding strategy problem based on the following modes of operation:

1. Uncoordinated operation of all three available energy resources.
2. Coordinated operation of two energy resources + Uncoordinated operation of the last energy resources.
3. Coordinated operation of all three available energy resources.

Note that the authors have passed up to present the formulation of the first and second trading strategies to avoid tautology in writing. It is notable that the superscript numbers in the constraints of the second strategy point out two distinct trading strategy in this case study.

Fig. 1 is placed here

### 2.3. Solution method of the multi-objective optimization problem

Most practical engineering issues are faced with more than one objective function, which in many cases, these objective functions conflict with each other. Multifarious techniques and methods have been employed in the literature to solve multi-objective problems, which $\epsilon$-constraint technique [20] and the weighted sum (WS) approach [24] are among these methods. In the present paper, the weighted sum technique has been used to solve the multi-objective bidding strategy of wind-thermal-photovoltaic energy resources. In the weighted sum method, all objective functions with different weighting factors that represent the relative significance of each objective function are put together in a separate objective function according to the following equation:

$$\text{Min } \; [OF] = w_1 F_1^{'} + w_2 F_2 \tag{28}$$

subject to

$$\begin{cases} w_1 + w_2 = 1 \\ F_1^{'} = -F_1 \\ \text{All restrictions of the proposed probelm} \end{cases} \tag{29}$$

where $F_1$ and $F_2$ stand for the two conflicting objective functions of the proposed problem, i.e., profit maximization and emission minimization. One of the problems faced by decision-makers in the weighted sum method is the different scale of objective functions in (28). To this end, a fuzzy satisfying approach is proposed to overcome this issue in the literature of multi-objective programming problems [21]. Based on this approach, the objective functions in (28) are normalized as follows:

$$\mathrm{F}_{1,\mathrm{pu}} = \frac{F_1 - F_1^{max}}{F_1^{max} - F_1^{min}} \tag{30}$$

$$\mathrm{F}_{2,\mathrm{pu}} = \frac{F_2^{max} - F_2}{F_2^{max} - F_2^{min}} \tag{31}$$

where $F_{1,pu}$ and $F_{2,pu}$ are the per unit values of objective functions $F_1$ and $F_2$, respectively. In fact, the equations (30) and (31) map the objective functions $F_1$ and $F_2$ in the range 0 and 1. $(F_1^{max}, F_2^{max})$ and $\left(F_1^{min}, F_2^{min}\right)$ represent the obtained maximum and minimum values of each objective function through the single objective optimization process, respectively. After normalizing each objective function, the objective function of the weighted sum method is rewritten as follows:

$$\mathrm{Min} \;\; [OF] = w_1 \mathrm{F}^{'}_{1,\mathrm{pu}} + w_2 \mathrm{F}_{2,\mathrm{pu}} \tag{32}$$

### *2.4. Decision-maker's approach to select the best compromise solution*

After obtaining the Pareto solutions via the WS method, the most favored solution among all set of solutions should be picked up. In the present paper, the final selection of the best compromise solution is accomplished based on the mindset, inclination, and preferences of decision-makers [25]. Indeed, decision-makers ascertain the minimum and maximum permissible values for the objective functions based on insight, the experience of previous years, short-term and long-term plans, and restrictions imposed by system operators. In this regard, for the objective function of maximizing profit, the minimum acceptable profit and for the objective function of minimizing emission, the maximum allowable emission is determined by the decision-maker, and finally, the most favored solution is selected based on these preconditions.

### *2.5. Uncertainty characterization*

The uncertain sources in the optimal bidding strategy of a GenCo are generally divided into two groups: the price of various target markets and generation power of renewable energy sources. The methodology for modeling the uncertainties arising from electricity market prices and output power of renewable energy sources will be explained in the following subsections.

*2.5.1. Market Prices uncertainty model*

In the proposed framework, the normal probability density function (PDF) is utilized to model the three uncertain market prices: the day-ahead energy and spinning reserve market prices along with the real-time market price. The PDF of an electricity market price $\lambda_{price}$ with mean $\mu_{price}$ and standard deviation $\sigma_{price}$ would be formulated as follows:

$$f_{price}(\lambda_{price}, \mu_{price}, \sigma_{price}) = \frac{1}{\sigma_{price}\sqrt{2\pi}} exp\left[-\frac{(\lambda_{price} - \mu_{price})^2}{2\sigma_{price}^2}\right] \tag{33}$$

*2.5.2. Wind power uncertainty model*

As it is evident, the production power of a wind turbine is not constant and changes as a function of wind speed. In the current paper, the Weibull PDF has been considered for modeling wind speed. The Weibull PDF of wind speed $V$ with scale and shape factors $c$ and $k$ is defined as follows:

$$f_{wind}(V, c, k) = \frac{k}{c}\left(\frac{V}{c}\right)^{k-1} exp\left[-\left(\frac{V}{c}\right)^{k}\right] \tag{34}$$

The generated power of a wind turbine in specified wind speed $V$ has fully corresponded to its technical specifications, namely, cut-out speed $v_{co}$, cut-in speed $v_{ci}$, and rated speed $v_r$, which is calculated using the following equation:

$$P_{wind} = \begin{cases} 0, & 0 \leq V \leq v_{ci} \\ P_{rated} \times \left(\frac{V - v_{ci}}{v_r - v_{ci}}\right), & v_{ci} \leq V \leq v_r \\ P_{rated}, & v_r \leq V \leq v_{co} \end{cases} \tag{35}$$

*2.5.3. Solar power uncertainty model*

Solar irradiance is the most significant factor in determining the output power of photovoltaic units, which is always confronted with uncertainties. In this paper, the Beta PDF is utilized as an appropriate expression pattern of solar irradiance. The Beta PDF of solar irradiance $Si$ is expressed as follows:

$$f_{irr}(Si, \alpha, \beta) = \begin{cases} \frac{\Gamma(\alpha+\beta)}{\Gamma(\alpha)\Gamma(\beta)} \times (Si)^{\alpha-1} \times (1-Si)^{\beta-1}, & 0 \leq Si \leq 1, \alpha \geq 0, \beta \geq 0 \\ 0, & otherwise \end{cases} \tag{36}$$

Given the solar irradiance $Si$ of photovoltaic units, their efficiency $\eta^{PV}$ and total area $S^{PV}$, the output power of PV units $P_{PV}$ are calculated as follows [23]:

$$P_{PV} = \eta^{PV} \times S^{PV} \times Si \tag{37}$$

Finally, By assigning appropriate probability density functions to each uncertain parameter, scenarios associated with these parameters are constructed by the roulette wheel mechanism [23].

## 3. Emission trading

In this paper, a solution fits the purchasing or selling emission quotas is presented for those occasions that taking advantage of emission trading is accessible for GenCos/industrial consumers. In this regard, [26] and [27] have focused on the detailed investigation of emission trading pattern in China's container terminal and building materials industry, respectively. Based on this approach, after solving the multi-objective bidding strategy problem, a specific strategy for each Pareto optimal solution will be adopted. If the emission of thermal units per Pareto exceeds the emission quota, the GenCo will have to purchase additional emission quotas. However, if the emission of a GenCo in each Pareto is less than the assigned emission quota, the Genco can sell its surplus emission quota. As mentioned above, the total expected earnings of GenCo in every Pareto optimal solution will be calculated as follows:

$$TPF = EPP + \left[\lambda^{EM} \times \left(E^{EQ} - EEG\right)\right] \tag{38}$$

where the TPF is net expected profit, EPP is the expected profit of GenCo per Pareto, $E^{EQ}$ is the assigned emission quota to GenCo, $\lambda^{EM}$ refers to emission price, and the EEG stands for the expected emission of GenCo per Pareto. Ultimately, for each emission price, a Pareto with the maximum value of TEP is selected as the optimal Pareto solution of the proposed bidding strategy problem.

## 4. Results and discussion

### *4.1. Input data*

The proposed system under study comprises five thermal units, a wind farm, and a PV site with the maximum capacity of 340 MW, 250 MW, and 150 MW for each, respectively. The economic and technical information on thermal units is provided in Table 2 and Table 3. These data have been extracted with some adjustments from [16]. Also, the data related to the emission curve of thermal units are given in Table 4. It is worthwhile to mention again that the quadratic cost and emission curves of thermal units are approximated by three piecewise blocks. This action, along with the proper formulation of the problem, leads to the absence of any nonlinear term in the proposed issue. On the basis of previously published papers, the $SO_2$ and $NO_x$ are considered as the fundamental origins of emission [21]. The expected values of forecasted wind speed and solar irradiance [28] are portrayed in Fig. 2 while information on wind turbines and PV site are provided in Table 5.

Tables 2, 3, 4, and 5 are placed here

Figure 2 is placed here

In the proposed model, GenCo only allows the thermal units to participate in the spinning reserve market, and since the offer of each unit in this market has to be ready to deliver in ten minutes, the maximum offer for each unit in this market is calculated using $\mathrm{PS}^{\mathrm{Max}}(\mathrm{g}) = \frac{1}{6} \times \mathrm{RUR}(\mathrm{g})$ [29]. As outlined in subsection 2.5, five uncertainty sources exist in the proposed structure (day-ahead market, spinning reserve market, and imbalance prices as well as wind and PV generation). Based on the suggested model, for each parameter, the adequate number of scenarios based on the statistical analysis of [28] and [30] is constructed using roulette wheel mechanism, and with a common approach, i.e., fast forward reduction technique [16] and [19], the initially generated scenarios for each parameter are reduced to three representative scenarios. Consequently, the final scenario set will contain $3^5 = 243$ scenarios. The proposed structure is formulated based on the MIP and has been implemented in GAMS (general algebraic modeling system), with CPLEX as the solver.

### *4.2. Results*

In order to assess the performance of the proposed structure, two different case studies are considered in this paper. In the first case study, we examine the single objective framework for the bidding strategy of the system under consideration, and in the second case study, the multi-objective bidding strategy of the wind-thermal-PV system is discussed. It is worth to note that in all case studies, the three trading strategies shown in Fig. 1 is fully explored. The first trading strategy appertained to the disjoint operation of all three energy sources in the electricity markets. The second trading strategy refers to the coordinated operation of wind and thermal units, while the PV system individually and independently participates in the electricity market. Eventually, the third trading strategy relates to the coordinated operation of all available energy sources.

#### *4.2.1. Case study 1*

As already mentioned, this case study focuses on the single objective bidding strategy of the system under study. In other words, this case study focuses solely on maximizing producer's profit without having a program or goal to minimize emissions. The results of this case study have been exhibited in Table 6. It is necessary to mention that this table will allow us to compare the economic and environmental aspects of different trading strategies. According to the obtained results, trading strategy 1 has the lowest expected profit (€302434.636) and the highest imbalance cost (€25369.536) among all three trading strategies. In contrast, coordinated operations of all three resources (trading strategy 3) have resulted in the highest profitability and the lowest imbalance cost, which the obtained results are €304509.778 and €15278.357, respectively. Similarly, in the second trading strategy that includes the coordinated operation of wind and thermal resources, more profit (€303221.192) and fewer imbalance cost (€23037.277) are obtained compared to the first strategy. From a different point of view, coordinated operation of energy resources in the proposed bidding strategy not only increase the profitability of the power producer but also reduces the emission of thermal units. It has to be noted that the numeric percent for comparing the decreasing or increasing values related to expected profit, expected emission, and expected imbalance cost of trading strategies two and three will be presented later to check out the effectiveness of the proposed bidding strategy.

Table 6 is placed here

Fig. 3 shows the expected participation of WTPV system in the energy and spinning reserve markets for all trading strategies. According to Fig. 3a, it is observed that at almost most of the hours, trading strategy 1 has more participation in the energy market. This issue has led the trading strategy 1 to have the highest imbalance cost, which ultimately leads to more reduction in the expected profit of WTPV system. Besides, it can be viewed that the difference in the participation of various trading strategies in the day-ahead energy market reflects more during high market prices. On the other hand, as shown in Fig. 3b, the participation of WTPV system in the spinning reserve market for trading strategies 2 and 3 are similar at most hours. Also, the high day-ahead market prices during hours 11-14 have led to a reduction in producer's participation in the spinning reserve market for the specified time interval. In other words, the producer will have a greater willingness to participate in the energy market instead of participating in the spinning reserve market to gain more profit in the aforementioned time interval. Finally, Fig. 4 presents the comparison between the share of thermal units from the entire participation of WTPV system in the energy market for all trading strategies. The share of thermal units in trading strategies 1 and 2 are lower than the first trading strategy, which leads to lower emission of power producer, as reported in Table 6. It is worth mentioning that Fig. 3 and Fig. 4 are demonstrated to unfold how the coordinated trading strategy of various available sources will alter the expected participation of the whole system and thermal units in the energy and spinning reserve markets, respectively.

Figures 3 and 4 are placed here

### *4.2.2. Case study 2*

This case study is designed to address the multi-objective bidding strategy of the wind-thermal-PV system. Contrary to the first case study, in this case study, minimizing the emission of thermal units is also added to one of the decision-maker's goals in the optimization process. As discussed in the previous sections, the weighted sum method is used to solve the multi-objective optimization problem. In this method, different weighting factors for objective functions (here, w1 and w2) are chosen subject to w1+ w2 = 1, and finally, the Pareto solutions of the proposed problem will be obtained. The results of Pareto for trading Strategies 1, 2, and 3 are shown in Fig. 5, Fig. 6, and Fig. 7, respectively. After obtaining Pareto results, the proposed approach in subsection 2.4 is implemented to select the most favored solution among all Pareto solutions. The minimum and maximum predetermined limits for the profit and emission are assumed to be $20\times10^3$ lbs and € $250\times10^3$, respectively. It has to be noted that these limits are determined by the decision-maker (GenCo) to merely compare the results of different trading strategies under similar conditions and consequently, every other restriction can be imposed by the decision-maker. Accordingly, the presented Pareto solutions in Fig. 5, Fig. 6, and Fig. 7 will let us pick the most favored solution under different predetermined restrictions. The summary results of different trading strategies in terms of the environmental and economic evaluation of the multi-objective bidding strategy have been provided in Table 7. It is worth noting that the results of Table 7 correspond to the red box of Fig. 5, Fig. 6 and Fig. 7 ($P14$) that obtained through the suggested approach in subsection 2.4.

---

Table 7 is placed here

---

---

Figures 5, 6 and 7 are placed here

---

According to the provided results in Table 7, trading strategies 2 and 3 have also led to an increase in the producer's expected profit in the multi-objective bidding strategy. The expected profit for trading strategies one, two, and three is €253638.926, €255566.283, and €256978.704, respectively. In this regard, the most expected profit is achieved via the third trading strategy (€256978.704) Which is consistent with the results of the previous case study. Similar to the first case study, in the second case study, the trading strategies 2 and 3 also diminish the imbalance costs and emissions in comparison with the first trading strategy.

Similar to Fig. 3, Fig. 8 illustrates the expected bids of power producer that are going to be submitted in the energy and spinning reserve markets for all three trading strategies. The expected production bids in the energy market (Fig. 8a) follow the explanation given about Fig. 3a, with the difference that the rates of production bids are significantly reduced. Fig. 8b allows us to conclude that the power producer's bidding approach in the spinning reserve market for all trading strategies will not affect the producer's strategy in this market. This issue stems from the fact that the producer tends to utilize the maximum level of participation in the spinning reserve market to gain its expected profit in whole trading strategies while the pollution constraints restrict its production in the energy market. At the remaining hours, the rising level of GenCo's participation in the energy market, the GenCo's involvement in the spinning reserve also increases. Analogous to Fig. 4, the comparison between the portion of thermal units from the total participation of the WTPV system in the energy market for all trading strategies in the multi-objective optimization approach is captured in Fig. 9. In fact, this figure exposes how the emission of both trading strategies 2 and 3 will be reduced in comparison with the first trading strategy. In comparison with the first case study, a large portion of the thermal units' production bids has been reduced, which is more evident in time intervals with lower energy prices.

---

Figures 8 and 9 are placed here

---

In order to participate in diverse electricity markets, the producers should submit their bidding packages to each specific market. The bidding curves of the power producer in the energy market for hours 8 and 22 for both single-objective and bi-objective bidding approaches are captured in Fig. 10 and Fig. 11. It can be noticed that in the coordinated operation of energy resources, for example, trading strategy 3, a bidding curve from all three energy resources is submitted to the day-ahead energy market. As can be seen from these curves, the coordinated operation of two or all units (strategy 2 or 3) leads to a change in the producer's bidding curve compared to the uncoordinated one (strategy 1). This is evident for both single objective and bi-objective bidding approaches. Moreover, the drop in bid volumes of bi-objective bidding approach compared to the single objective one is noticeable as can be seen from these figures.

---

Figures 10 and 11 are placed here

---

In this paper, along with the proposed approach in subsection 2.4, emission trading is also taken into consideration as a new scheme in the decision-making process of the power producer. Following the explanations given in section 3, after solving the multi-objective bidding strategy problem and obtaining corresponding Pareto solutions, this approach is implemented to select the optimal solution among all Pareto solutions. The maximum TPF obtained by equation (38) will be the optimal solution corresponding to each emission price. One of the superiorities and advantages of this method versus other techniques is that the emission quota of the power producer is implicitly included in the bidding process. In the current paper, in order to avoid tautology in the demonstration of results, only the results of emission quota arbitraging for trading strategy 3 have been reported in Table 8. The emission quota of the power producer is considered $20 \times 10^3$ lbs. The bold numbers in each column pertaining to emission prices indicate the optimal Pareto solution for that particular emission price. As can be seen from this table, the increase in the price of emission leads to a reduction in the expected net profit of the power producer.

---

Table 8 is placed here

---

### *4.3. Discussion*

In the current paper, a comprehensive bidding model for the participation of wind, thermal, and photovoltaic units has been proposed. In summary, by examining the presented results in two case studies using the suggested approach in subsection 2.4, we can conclude that the proposed trading strategies will increase the expected profit and reduce the expected emission of the power producer. In order to assess the effectiveness of the second and third trading strategies in comparison with the first trading strategy, Fig. 12 and Fig. 13 are provided. According to these figures, it can be concluded that:

1. In both case studies, third trading strategy has the highest profit increment, which these values are 1.36% and 0.68% for the first and second case studies, respectively.

2. In both case studies of the second and third trading strategies, the emission of thermal units decreases compared to the first trading strategy, which is more striking in the first case study.

3. Trading strategy 3 has the highest imbalance reduction, especially in the bi-objective bidding approach.

4. Reducing the expected production bids in the energy market has led to a reduction in the cost of imbalances and, consequently, an increase in the producer's profit.

5. In the bi-objective bidding approach, the trading strategy of power producer will not affect the participation level of thermal units in the spinning reserve market.

---

Figures 12 and 13 are placed here

---

Nevertheless, two other items can be considered as further suggestions for the future research of authors in the bidding strategy of a WTPV system:

1. Considering a risk measuring index in the bi-objective bidding strategy of WTPV system as an additional parameter.

2. Proposing a bi-level bidding model for the WTPV system while it behaves as a price-maker producer in one of the target electricity markets.

## 5. Conclusion

In this paper, a new framework for multi-objective bidding strategy of an integrated wind-thermal-photovoltaic system alongside two different decision-making schemes was proposed to attain the introduced contributions. In order to assess the effectiveness of the suggested bidding structure, three different trading strategies, including coordinated and uncoordinated operation of generation units, along with their relevant formulation were comprehensively presented, and subsequently, an efficient technique was applied to solve the bi-objective problem. Based on the proposed bidding strategies, the coordinated operation of all energy resources was led to the highest expected profit in both single-objective and multi-objective bidding strategies. In fact, in the bi-objective model, the aim was to evaluate the profitability of the coordinated bidding strategy of all available sources in the presence of an additional objective function, which in this occasion, the proposed bidding strategy was also able to gain the total expected profit of the system. Also, the numerical results have demonstrated that reduction in the output power of thermal units in the bi-objective approach will lead to considerable imbalance reduction in comparison with the single-objective one which is considered as the main reason for the profitability of the recommended model. This imbalance reduction was accompanied by a reduction in the participation of the system in the energy market. Another important observation of this paper was that the variation in the trading approach of the system did not affect the bidding strategy in the spinning reserve market. Also, the numerical results illustrated that emission trading in the electricity markets results in higher values of expected profit compared to the markets without this capability.

## References

[1] De Andrade Guerra, J.B.S.O., Dutra, L., Schwinden, N.B.C., Andrade, S.F. De, 2015. Future scenarios and trends in energy generation in Brazil: Supply and demand and mitigation forecasts. J. Clean. Prod. https://doi.org/10.1016/j.jclepro.2014.09.082

[2] Ram, M., Child, M., Aghahosseini, A., Bogdanov, D., Lohrmann, A., Breyer, C., 2018. A comparative analysis of electricity generation costs from renewable, fossil fuel and nuclear sources in G20 countries for the period 2015-2030. J. Clean. Prod. 199, 687–704.

[3] Wesseh, P.K., Lin, B., 2017. Options for mitigating the adverse effects of fossil fuel subsidies removal in Ghana. J. Clean. Prod. https://doi.org/10.1016/j.jclepro.2016.09.214

[4] Zafar, M.W., Shahbaz, M., Hou, F., Sinha, A., 2019. From nonrenewable to renewable energy and its impact on economic growth: The role of research & development expenditures in Asia-Pacific Economic Cooperation countries. J. Clean. Prod. https://doi.org/10.1016/j.jclepro.2018.12.081

[5] Yin, G., Zhou, L., Duan, M., He, W., Zhang, P., 2018. Impacts of carbon pricing and renewable electricity subsidy on direct cost of electricity generation: A case study of China's provincial power sector. J. Clean. Prod. https://doi.org/10.1016/j.jclepro.2018.09.108

[6] Nie, P. yan, Chen, Y. hua, Yang, Y. cong, Wang, X.H., 2016. Subsidies in carbon finance for promoting renewable energy development. J. Clean. Prod. https://doi.org/10.1016/j.jclepro.2016.08.083

[7] Shi, X., Dini, A., Shao, Z., Jabarullah, N.H., 2019. Impacts of photovoltaic/wind turbine/microgrid turbine and energy storage system for bidding model in power system. J. Clean. Prod.

[8] Abedinia, O., Zareinejad, M., Doranehgard, M.H., Fathi, G., Ghadimi, N., 2019. Optimal offering and bidding strategies of renewable energy based large consumer using a novel hybrid robust-stochastic approach. J. Clean. Prod. 215, 878–889.

[9] Aliasghari, P., Mohammadi-Ivatloo, B., Alipour, M., Abapour, M., Zare, K., 2018. Optimal scheduling of plug-in electric vehicles and renewable micro-grid in energy and reserve markets considering demand response program. J. Clean. Prod. https://doi.org/10.1016/j.jclepro.2018.03.058

[10] Tan, M., Chen, Y., Su, Y. xin, Li, S. hu, Li, H., 2019. Integrated optimization model for industrial self-generation and load schedul-

ing with tradable carbon emission permits. J. Clean. Prod. https://doi.org/10.1016/j.jclepro.2018.11.005

[11] Khaloie, H., Abdollahi, A., Rashidinejad, M., Siano, P., 2019. Risk-based probabilistic-possibilistic self-scheduling considering high-impact low-probability events uncertainty. Int. J. Electr. Power Energy Syst. 110, 598–612. https://doi.org/10.1016/j.ijepes.2019.03.021

[12] Perković, L., Mikulčić, H., Duić, N., 2018. Multi-objective optimization of a simplified factory model acting as a prosumer on the electricity market. J. Clean. Prod. https://doi.org/10.1016/j.jclepro.2016.12.078

[13] Hooshmand, R.A., Nosratabadi, S.M., Gholipour, E., 2018. Event-based scheduling of industrial technical virtual power plant considering wind and market prices stochastic behaviors - A case study in Iran. J. Clean. Prod. https://doi.org/10.1016/j.jclepro.2017.12.017

[14] Varkani, A.K., Daraeepour, A., Monsef, H., 2011. A new self-scheduling strategy for integrated operation of wind and pumped-storage power plants in power markets. Appl. Energy 88, 5002–5012. https://doi.org/10.1016/j.apenergy.2011.06.043

[15] Esmaeily, A., Ahmadi, A., Raeisi, F., Ahmadi, M.R., Esmaeel Nezhad, A., Janghorbani, M., 2017. Evaluating the effectiveness of mixed-integer linear programming for day-ahead hydro-thermal self-scheduling considering price uncertainty and forced outage rate. Energy 122, 182–193. https://doi.org/10.1016/j.energy.2017.01.089

[16] Al-Awami, A.T., El-Sharkawi, M.A., 2011. Coordinated trading of wind and thermal energy. IEEE Trans. Sustain. Energy 2, 277–287. https://doi.org/10.1109/TSTE.2011.2111467

[17] Lakshmi, K., Vasantharathna, S., 2014. Gencos wind–thermal scheduling problem using Artificial Immune System algorithm. Int. J. Electr. Power Energy Syst. 54, 112–122. https://doi.org/10.1016/j.ijepes.2013.06.036

[18] Laia, R., Pousinho, H.M.I., Melíco, R., Mendes, V.M.F., 2016. Bidding strategy of wind-thermal energy producers. Renew. Energy 99, 673–681. https://doi.org/10.1016/j.renene.2016.07.049

[19] Al-Swaiti, M.S., Al-Awami, A.T., Khalid, M.W., 2017. Co-optimized trading of wind-thermal-pumped storage system in energy and regulation markets. Energy 138, 991–1005. https://doi.org/10.1016/j.energy.2017.07.10

[20] Aghaei, J., Alizadeh, M.I., 2013. Multi-objective self-scheduling of CHP (combined heat and power)-based microgrids considering demand response programs and ESSs (energy storage systems). Energy 55, 1044–1054. https://doi.org/10.1016/j.energy.2013.04.048

[21] Ahmadi, A., Aghaei, J., Shayanfar, H.A., Rabiee, A., 2012. Mixed integer programming of multiobjective hydro-thermal self scheduling. Appl. Soft Comput. J. 12, 2137–2146. https://doi.org/10.1016/j.asoc.2012.03.020

[22] Simab, M., Javadi, M.S., Nezhad, A.E., 2018. Multi-objective programming of pumped-hydro-thermal scheduling problem using normal boundary intersection and VIKOR. Energy 143, 854–866. https://doi.org/10.1016/j.energy.2017.09.144

[23] Niknam, T., Kavousifard, A., Aghaei, J., 2012. Scenario-based multiobjective distribution feeder reconfiguration considering wind power using adaptive modified particle swarm optimisation. IET Renew. Power Gener. 6, 236–247.

[24] Jannati, J., Nazarpour, D., 2019. Optimal performance of electric vehicles parking lot considering environmental issue. J. Clean. Prod. 206, 1073–1088.

[25] Zakariazadeh, A., Jadid, S., Siano, P., 2014. Stochastic multi-objective operational planning of smart distribution systems considering demand response programs. Electr. Power Syst. Res. 111, 156–168.

[26] Zhong H, Hu Z, Yip TL. Carbon emissions reduction in China's container terminals: Optimal strategy formulation and the influence of carbon emissions trading. J Clean Prod 2019;219:518–30.

[27] Zhao, S., Shi, Y., Xu, J., 2018. Carbon emissions quota allocation based equilibrium strategy toward carbon reduction and economic benefits in China's building materials industry. J. Clean. Prod. 189, 307–325.

[28] Weather history+ - meteoblue [WWW Document], n.d. URL https://www.meteoblue.com/en/historyplus (accessed 4.22.19).

[29] Khaloie, H., Abdollahi, A., Rashidineiad, M., 2018. Risk-Constrained Self-Scheduling and Forward Contracting Under Probabilistic-Possibilistic Uncertainties, in: Electrical Engineering (ICEE), Iranian Conference On. IEEE, pp. 1138–1143. https://doi.org/10.1109/ICEE.2018.8472668.

[30] Bienvenido — ESIOS electricidad · datos · transparencia [WWW Document], n.d. URL https://www.esios.ree.es/es (accessed 3.14.19).

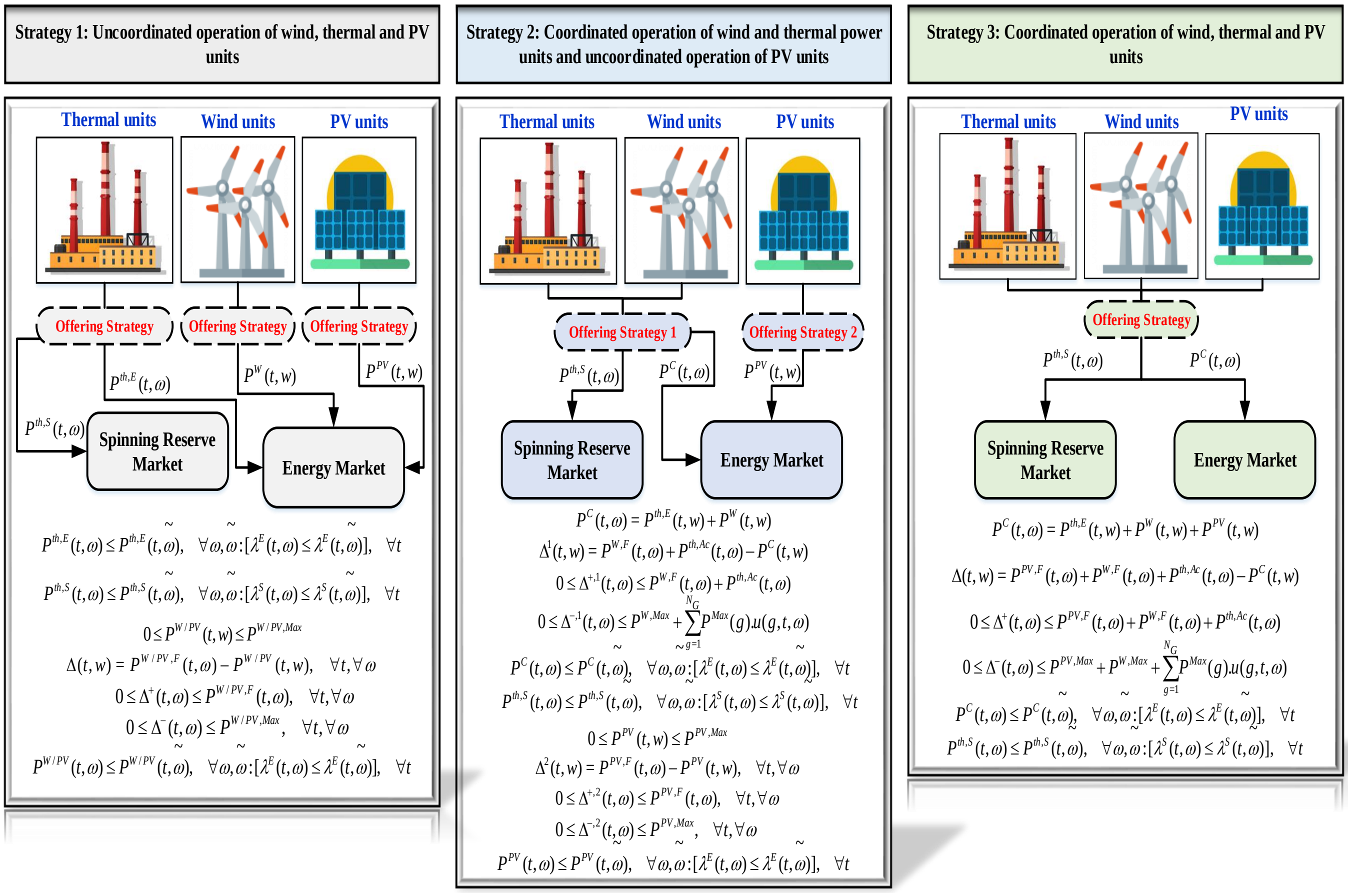


Figure 1: Schematic of different bidding strategies

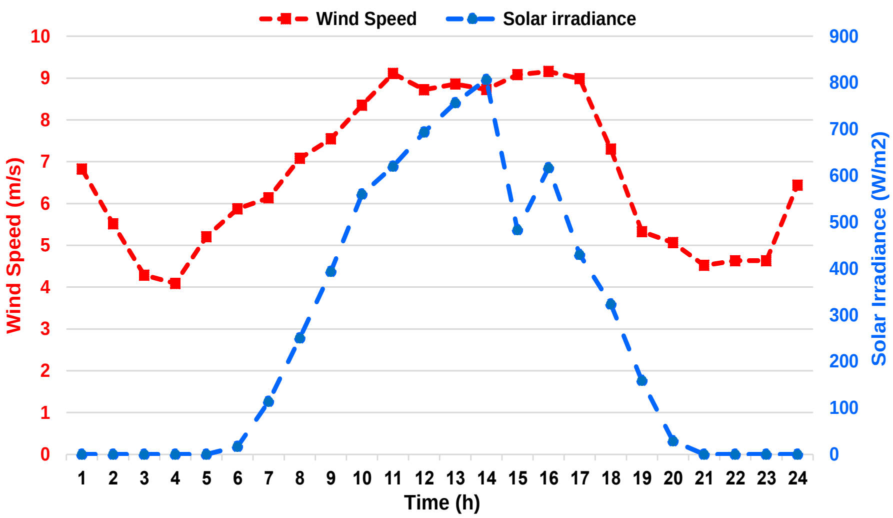


Figure 2: Expected values for hourly wind speed and solar irradiance

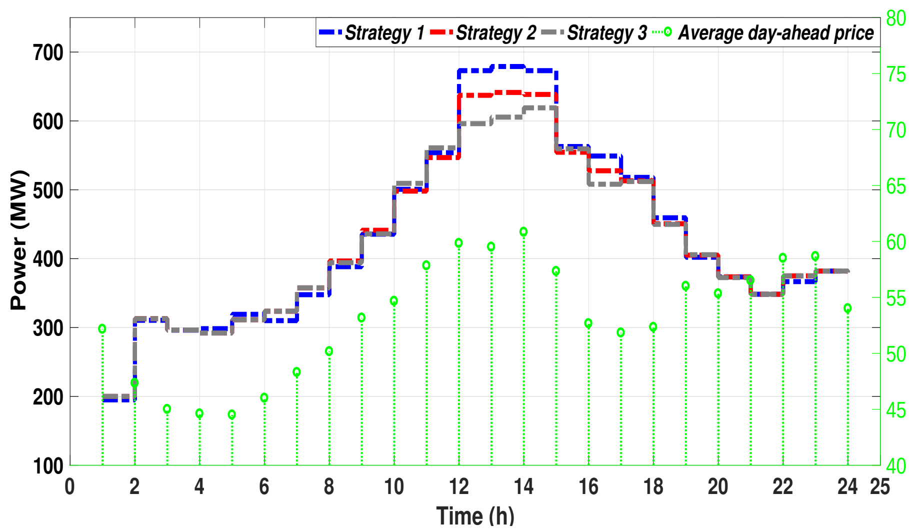


(a) Expected participation in the day-ahead energy market in different trading strategies

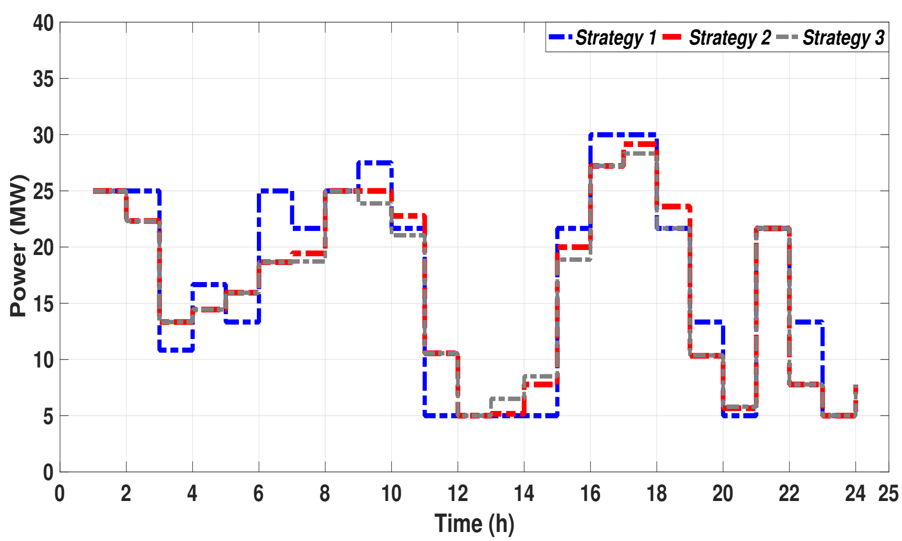


(b) Expected participation in the spinning reserve market in different trading strategies

Figure 3: Single objective bidding approach

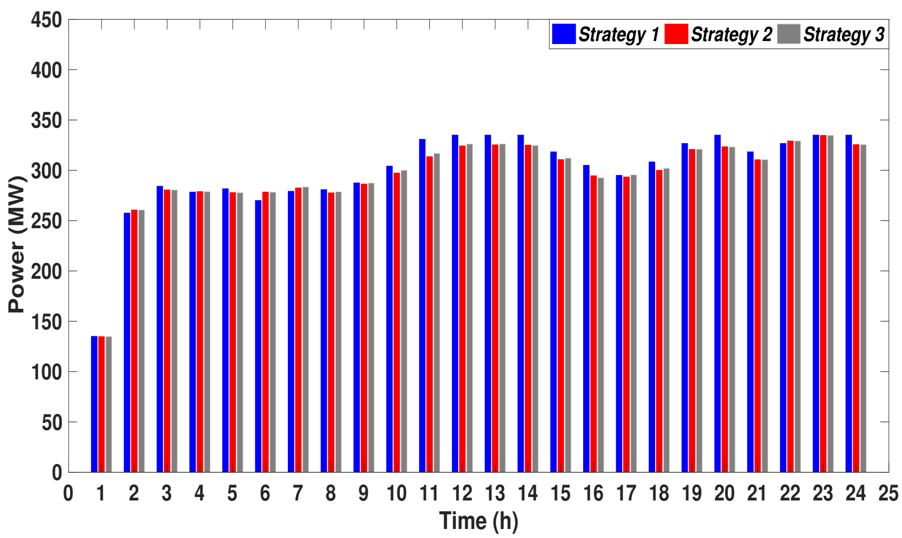


Figure 4: Comparison of expected amount of production bids of thermal units in the day-ahead energy market for all trading strategies (case study 1)

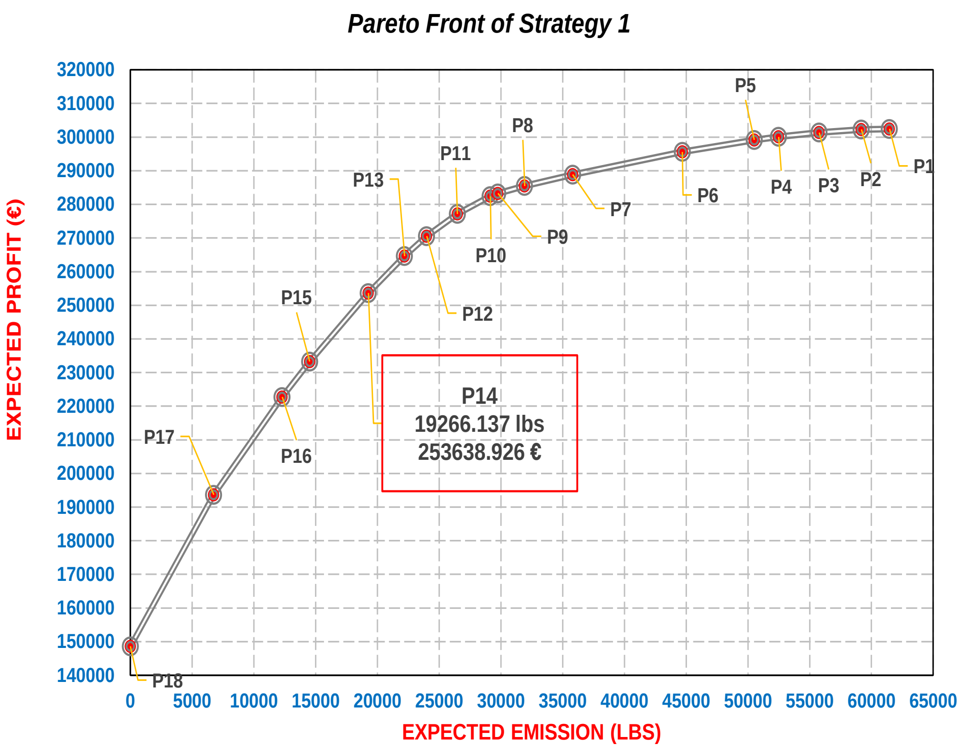


Figure 5: Pareto front for trading strategy 1

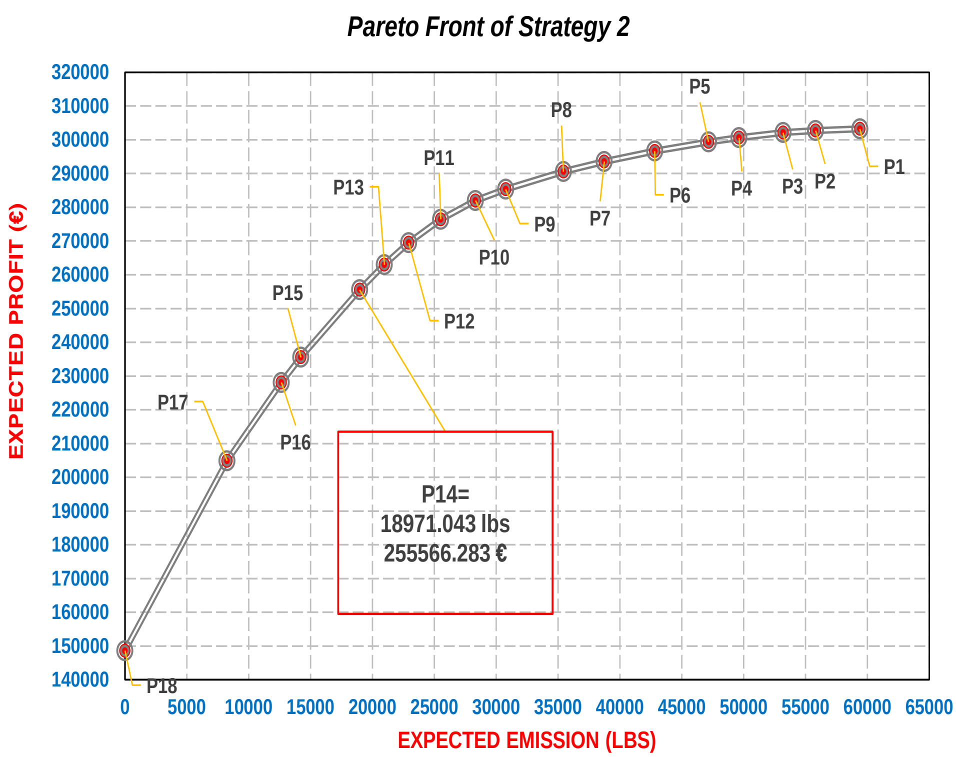


Figure 6: Pareto for trading strategy 2

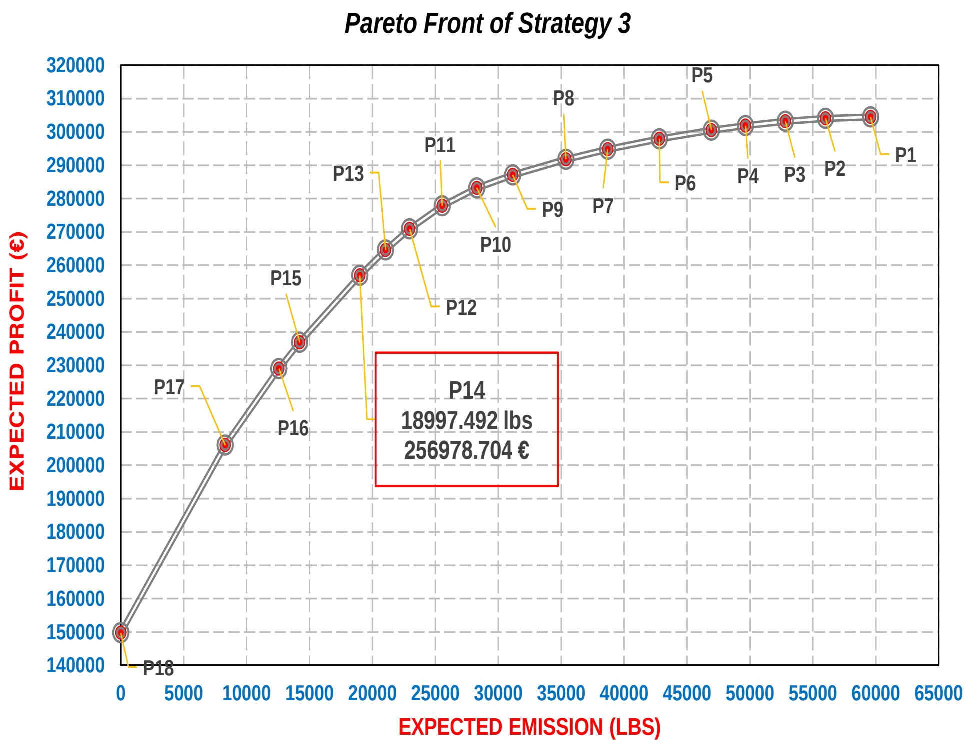


Figure 7: Pareto front for trading strategy 3

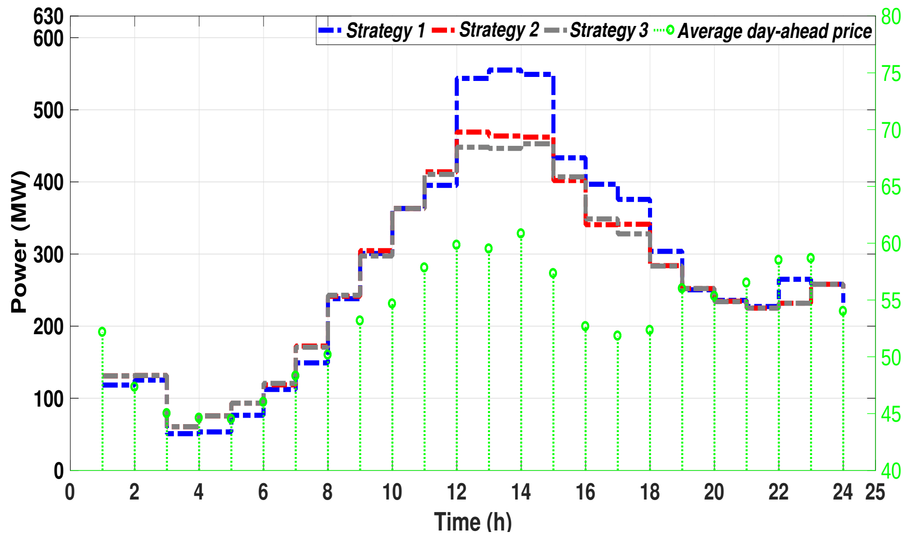


(a) Expected participation in the day-ahead energy market in different trading strategies

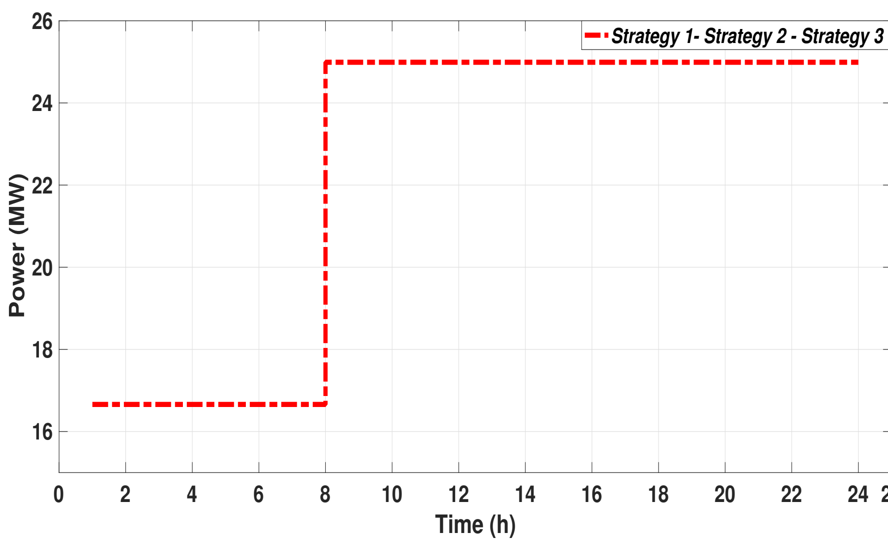


(b) Expected participation in the spinning reserve market in different trading strategies

Figure 8: Multi-objective bidding approach

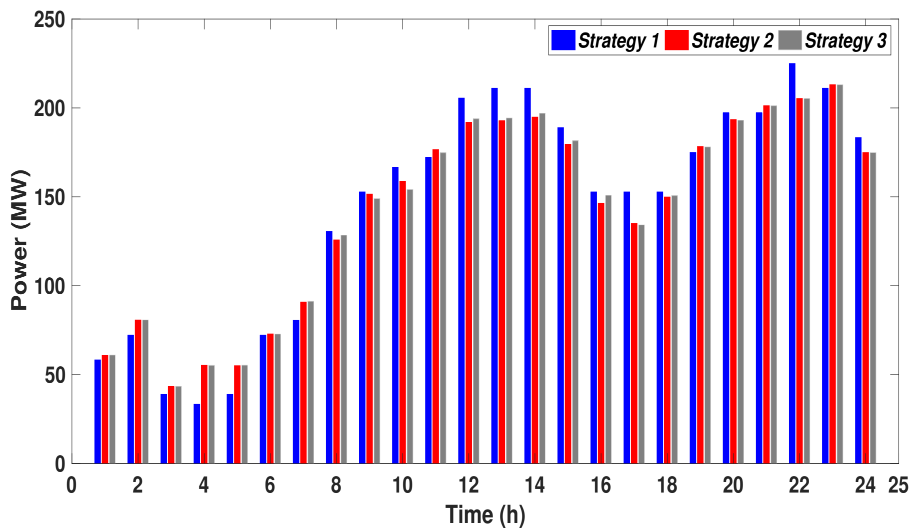


Figure 9: Comparison of expected amount of production bids of thermal units in the day-ahead energy market for all trading strategies (case study 2)

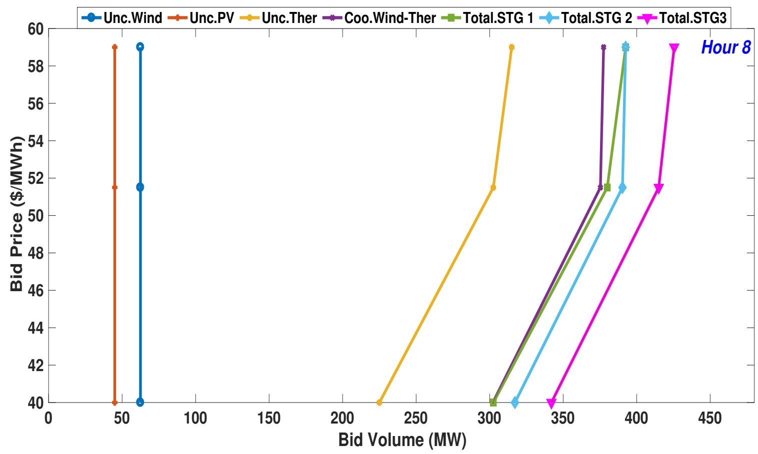


(a) Single objective bidding approach

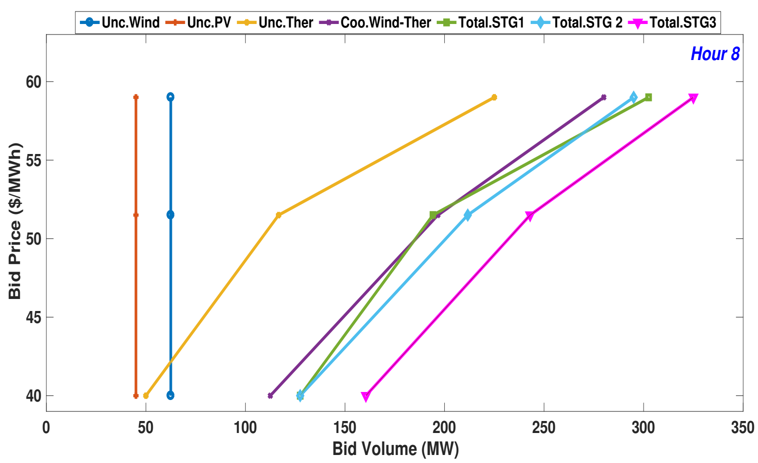


(b) Multi-objective bidding approach

Figure 10: Day-ahead energy market bidding for hour 8

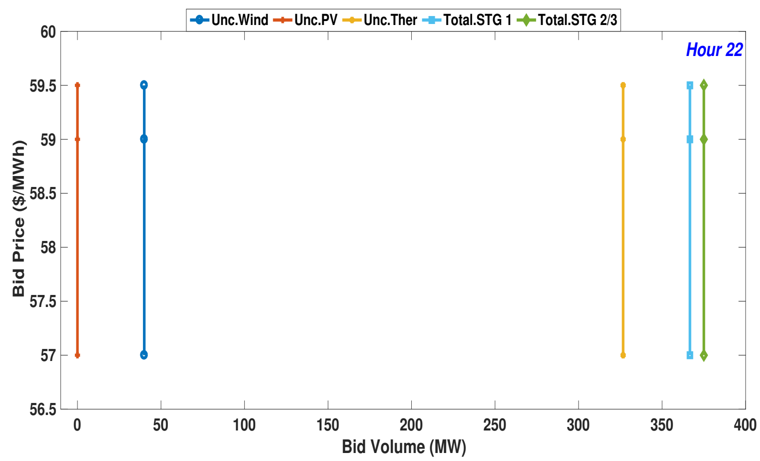


(a) Single objective bidding approach

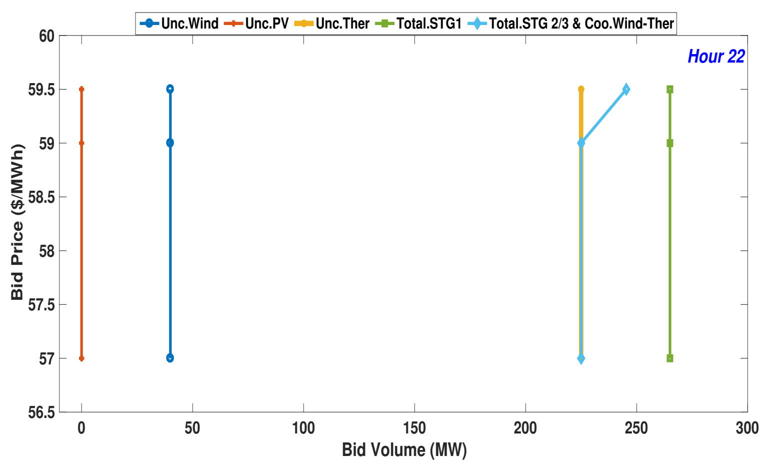


(b) Multi-objective bidding approach

Figure 11: Day-ahead energy market bidding for hour 22

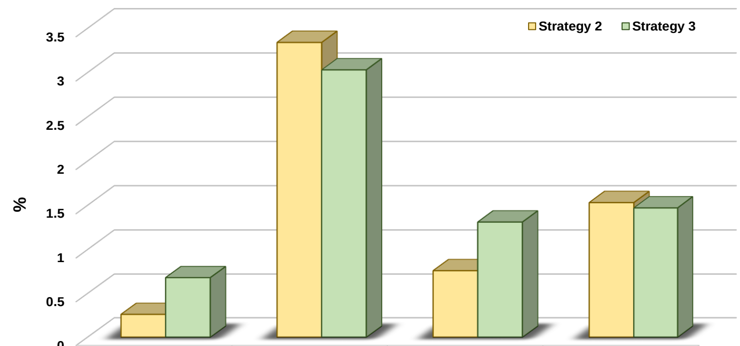


| | Profit Increment Single Objective | Emission Reduction Single Objective | Profit Increment Multi-Objective | Emission Reduction Multi-Objective |
|---|---|---|---|---|
| Strategy 2 | 0.26 | 3.34 | 0.76 | 1.53 |
| Strategy 3 | 0.68 | 3.03 | 1.31 | 1.47 |

(a) Profit increment and emission reduction in both case studies

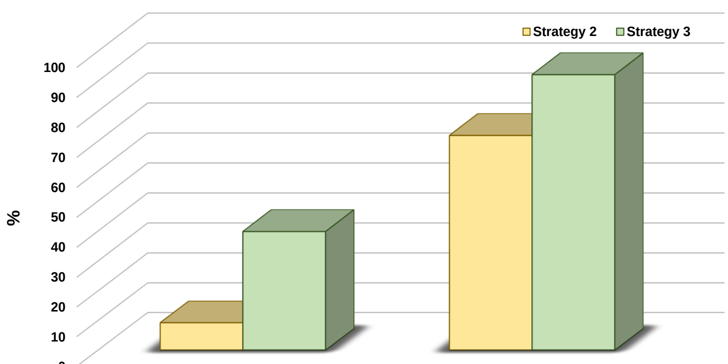


| | Imbalance Reduction Single Objective | Imbalance Reduction Multi-Objective |
|---|---|---|
| Strategy 2 | 9.19 | 71.82 |
| Strategy 3 | 39.77 | 92.1 |

(b) Imbalance reduction in both case studies

Figure 12: Comparison of profit increment, emission and imbalance reductions in the second and third trading strategies

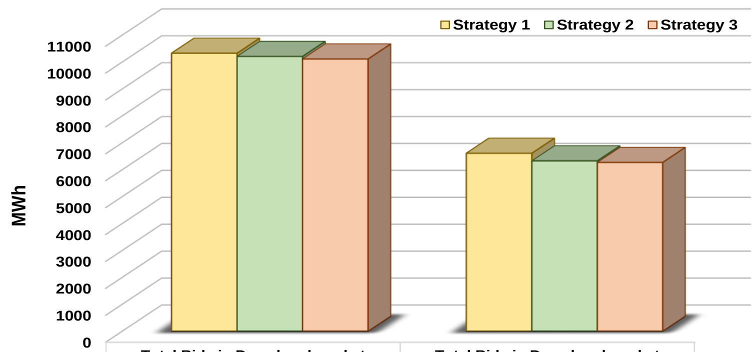


| | Total Bids in Day-ahead market (Single Objective) | Total Bids in Day-ahead market (Multi-Objective) |
|---|---|---|
| Strategy 1 | 10322.573 | 6605.643 |
| Strategy 2 | 10203.193 | 6322.643 |
| Strategy 3 | 10107.323 | 6264.84 |

(a) Expected total bids in the day-ahead energy market for both case studies

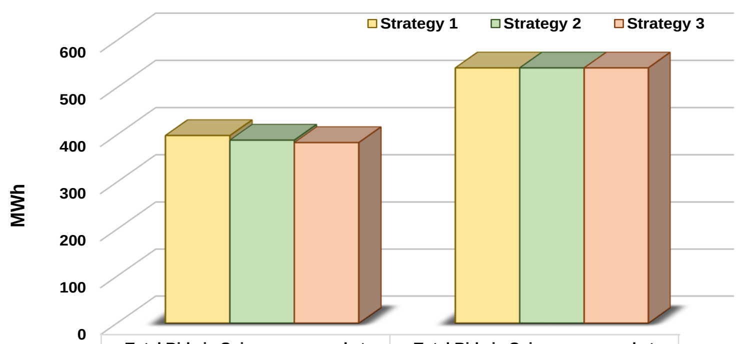


| | Total Bids in Spin.reserve market (Single Objective) | Total Bids in Spin.reserve market (Multi-Objective) |
|---|---|---|
| Strategy 1 | 398.21 | 541.45 |
| Strategy 2 | 388.54 | 541.45 |
| Strategy 3 | 383.325 | 541.45 |

(b) Expected total bids in the spinning reserve market for both case studies

Figure 13: Comparison of expected total day-ahead energy and spinning reserve bids in different trading strategies

Table 1: Taxonomy of the reviewed papers

| Ref. | Combination of Various Energy Sources | Problem Type | Uncertain Parameters | | | | | Uncertainty Modeling | Objective Functions | Solution Methodology of MOP |
|---|---|---|---|---|---|---|---|---|---|---|
| | | | EM | SPRM | BM | REP | OS | | | |
| [7] | Large consumer | BS | √ | — | — | √ | √ | SP-RO | CSM | — |
| [8] | Large consumer | BS | √ | — | — | √ | √ | SP-RO | CSM | — |
| [9] | Microgrid | SS | √ | √ | — | √ | √ | SP | CSM | — |
| [10] | Industrial Plant | SS | — | — | — | — | — | — | CSM | — |
| [11] | Thermal | SS | √ | √ | — | √ | √ | PP | PFM | — |
| [12] | Large consumer | SS | — | — | — | — | — | — | CSM+ICM | WSM |
| [13] | VPP | SS | √ | √ | — | √ | √ | SP | PFM | — |
| [14] | Wind-PSP | SS | — | — | — | √ | — | SP | PFM | — |
| [15] | Hydro-thermal | SS | √ | √ | — | — | √ | SP | PFM | — |
| [16] | Wind-thermal | BS | √ | — | — | √ | — | SP | PFM | — |
| [17] | Wind-thermal | SS | — | — | √ | — | — | — | PFM | — |
| [18] | Wind-thermal | BS | √ | — | — | √ | — | SP | PFM | — |
| [19] | Wind-thermal-PSP | BS | √ | — | √ | √ | √ | SP | PFM | — |
| [20] | Microgrid | SS | — | — | √ | — | — | — | CSM+EMM | EPM |
| [21] | Hydro-thermal | SS | — | — | — | — | — | — | PFM+EMM | EPM |
| [22] | Hydro-thermal-PSP | EED | — | — | — | — | √ | SP | CSM+EM | NBIM |
| **This paper** | **Wind-thermal-PV** | **BS** | √ | √ | √ | √ | — | **SP** | **PFM+EMM** | **WSM+FSA** |

*Note* : EM-Energy market; SPRM-Spinning reserve market; BM-Balancing market; REP-Renewable production; OS-Other sources; MOP-Multi-objective programming; PSP-Pumped storage Plant; VPP-Virtual Power Plant; MG-Microgrid; PV-Photovoltaic; BS-Bidding strategy; SS-Self-Scheduling; EED-Economic emission dispatch; SP-Stochastic programming; RO-Robust optimization; PP-Probabilistic possibilistic; PFM-Profit maximization; CSM-Cost minimization; EMM-Emission minimization; ICM-Investment cost minimization;WSM-Weighted sum method; WSM+FSA-Weighted sum method+Fuzzy satisfying approach; EPM-Epsilon Constraint method; NBIM-Normal boundary intersection method

Table 2: Thermal units information

| Thermal Units | Cost coefficients of generator | | | $P_{min}$ (MW) | $P_{max}$ (MW) |
|---|---|---|---|---|---|
| | $a_g$(€/$MW^2$h) | $b_g$(€/MWh) | $c_g$(€/h) | | |
| G1 | 0.0144 | 31.400 | 40.260 | 0 | 50 |
| G2 | 0.0339 | 43.022 | 85.509 | 5 | 45 |
| G3 | 0.0339 | 42.022 | 82.342 | 5 | 45 |
| G4 | 0.0330 | 28.090 | 42.760 | 25 | 100 |
| G5 | 0.0248 | 26.504 | 49.140 | 25 | 100 |

Table 3: Technical specification of thermal units

| Thermal units | RDR(g) (MW/hr) | RUR(g) (MW/hr) | STDRL(g) (MW/hr) | STURL(g) (MW/hr) | STUC(g) (€) |
|---|---|---|---|---|---|
| G1 | 50 | 50 | 30 | 20 | 0 |
| G2 | 15 | 15 | 20 | 15 | 88 |
| G3 | 15 | 15 | 20 | 15 | 88 |
| G4 | 50 | 50 | 60 | 50 | 110 |
| G5 | 50 | 50 | 60 | 50 | 110 |

Table 4: Emission coefficients of thermal units

| Thermal units | Coefficient of $SO_2$ emission function | | | Coefficient of $NO_x$ emission function | | |
|---|---|---|---|---|---|---|
| | $\alpha_g$ (lbs/$MW^2$) | $\beta_g$ (lbs/MW) | $\gamma_g$ (lbs) | $\alpha_g$ (lbs/$MW^2$) | $\beta_g$ (lbs/MW) | $\gamma_g$ (lbs) |
| G1 | 0.0249 | 3.554 | 1.866 | 0.0087 | 1.345 | 3.716 |
| G2 | 0.0167 | 12.259 | 4.470 | 0.0073 | 5.945 | 5.298 |
| G3 | 0.0167 | 11.259 | 4.470 | 0.0073 | 5.945 | 5.298 |
| G4 | 0.0157 | 2.762 | 2.262 | 0.0095 | 0.820 | 4.653 |
| G5 | 0.0157 | 2.762 | 2.262 | 0.0095 | 0.820 | 4.653 |

Table 5: Information on wind turbines and PV site

| Parameter | Value | unit | Parameter | Value | unit |
|---|---|---|---|---|---|
| $v_{ci}$ | 3 | m/s | $\eta^{PV}$ | 15 | % |
| $v_r$ | 15 | m/s | $S^{PV}$ | $10^6$ | $m^2$ |
| $v_{co}$ | 25 | m/s | $P^{PV}_{rated}$ | 150 | MW |
| $P^W_{rated}$ | 250 | MW | - | - | - |

Table 6: Results of single objective bidding strategy in various trading strategies

| Trading strategy | Expected profit (€) | Expected emission (lbs) | Imbalance cost (€) |
|---|---|---|---|
| Wind uncoordinated | 94868.919 | — | 16995.914 |
| PV uncoordinated | 53734.278 | — | 8373.622 |
| Thermal uncoordinated | 153831.439 | 61455.848 | — |
| Sum uncoordinate wind and thermal | 248700.358 | 61455.848 | 16955.914 |
| Coordinated wind and thermal | 249486.914 | 59401.666 | 14663.655 |
| Sum uncoordinated wind, PV and thermal (Strategy 1) | 302434.636 | 61455.848 | 25369.536 |
| Sum uncoordinated PV and coordinated wind-thermal (Strategy 2) | 303221.192 | 59401.666 | 23037.277 |
| Sum coordinate wind, PV and Thermal (Strategy 3) | 304509.778 | 59590.001 | 15278.357 |

Table 7: Results of Multi-objective bidding strategy in various trading strategies

| Trading strategy | Expected profit (€) | Expected emission (lbs) | Imbalance cost (€) |
|---|---|---|---|
| Wind uncoordinated | 94868.919 | — | 16995.914 |
| PV uncoordinated | 53734.278 | — | 8373.622 |
| Thermal uncoordinated | 105035.729 | 19266.137 | — |
| Sum uncoordinate wind and thermal | 199904.648 | 19266.137 | 16955.914 |
| Coordinated wind and thermal | 201832.005 | 18971.043 | -1225.947 |
| Sum uncoordinated wind, PV and thermal (Strategy 1) | 253638.926 | 19266.137 | 25369.536 |
| Sum uncoordinated PV and coordinated wind-thermal (Strategy 2) | 255566.283 | 18971.043 | 7147.675 |
| Sum coordinate wind, PV and Thermal (Strategy 3) | 256978.704 | 18997.492 | 2003.541 |

Table 8: Results of emission quota arbitraging for Pareto optimal solutions of strategy 3

| Total Emission (lbs) | Profit without emission trade (€) | Emission trades (lbs) | Net profits (€) | | | |
|---|---|---|---|---|---|---|
| | | | $\lambda^{EM}$=0.1 (€/lbs) | $\lambda^{EM}$=0.3 (€/lbs) | $\lambda^{EM}$=0.5 (€/lbs) | $\lambda^{EM}$=1 (€/lbs) |
| 59590.001 | 304509.778 | -39590.001 | **300550.778** | 292632.778 | 284714.778 | 264919.777 |
| 56009.132 | 304058.522 | -36009.132 | 300457.608 | 293255.782 | 286053.956 | 268049.390 |
| 52814.999 | 303192.137 | -32814.990 | 299910.637 | **293347.637** | 286784.638 | 270377.147 |
| 49652.657 | 301854.928 | -29652.657 | 298889.662 | 292959.131 | 287028.600 | 272202.271 |
| 46939.804 | 300526.825 | -26939.804 | 297832.845 | 292444.884 | **287056.923** | 273587.021 |
| 42807.933 | 297896.198 | -22807.933 | 295615.405 | 291053.818 | 286492.232 | 275088.265 |
| 38700.833 | 294798.142 | -18700.833 | 292928.059 | 289187.892 | 285447.726 | 276097.309 |
| 35374.524 | 291777.572 | -15374.524 | 290240.120 | 287165.215 | 284090.310 | **276403.048** |
| 31145.031 | 287088.975 | -11145.031 | 285974.472 | 283745.466 | 281516.460 | 275943.944 |
| 28286.335 | 283176.988 | -8286.335 | 282348.355 | 280691.088 | 279033.821 | 274890.653 |
| 25544.215 | 277774.429 | -5544.215 | 277220.008 | 276111.165 | 275002.322 | 272230.214 |
| 22952.056 | 270843.444 | -2952.056 | 270548.238 | 269957.827 | 269367.416 | 267891.388 |
| 21044.007 | 264561.387 | -1044.007 | 264456.986 | 264248.185 | 264039.384 | 263517.380 |
| 18997.492 | 256978.704 | 1002.508 | 257078.955 | 257279.456 | 257479.958 | 257981.212 |
| 14221.486 | 236828.236 | 5778.514 | 237406.087 | 238561.790 | 239717.493 | 242757.218 |
| 12567.015 | 229008.445 | 7432.985 | 229751.744 | 231238.341 | 232724.938 | 236441.430 |
| 8303.996 | 206041.240 | 11696.004 | 207210.840 | 209550.041 | 211889.242 | 217737.244 |
| 0 | 149735.991 | 20000.000 | 151735.991 | 155735.991 | 159735.991 | 169735.991 |